Polymer-induced phase separation in suspensions of bacteria

Polymer-induced phase separation in suspensions of bacteria

2010 EPL 89 68003

(http://iopscience.iop.org/0295-5075/89/6/68003)

A Letters Journal Exploring the Frontiers of Physics

March 2010

EPL, **89** (2010) 68003 www.epljournal.org
doi: 10.1209/0295-5075/89/68003

Polymer-induced phase separation in suspensions of bacteria

J. Schwarz-Linek[1], G. Dorken[1,2], A. Winkler[3], L. G. Wilson[1], N. T. Pham[1], C. E. French[2], T. Schilling[3(a)] and W. C. K. Poon[1(b)]

[1] *SUPA and School of Physics & Astronomy, The University of Edinburgh, James Clerk Maxwell Building, Kings Buildings - Mayfield Road, Edinburgh EH9 3JZ, UK, EU*
[2] *Institute for Cell Biology, School of Biological Sciences, The University of Edinburgh, Darwin Building, Kings Buildings - Mayfield Road, Edinburgh EH9 3JR, UK, EU*
[3] *Institut für Physik, Johannes Gutenberg Universität - 55099 Mainz, Germany, EU*

received 8 January 2010; accepted in final form 10 March 2010
published online 19 April 2010

PACS 82.70.Dd – Colloids
PACS 87.18.Ed – Cell aggregation
PACS 87.18.Fx – Multicellular phenomena, biofilms

Abstract – We study phase separation in suspensions of two unrelated species of rod-like bacteria, *Escherichia coli* and *Sinorhizobium meliloti*, induced by the addition of two different anionic polyelectrolytes, sodium polystyrene sulfonate or succinoglycan, the former being synthetic and the latter of natural origin. Comparison with the known behaviour of synthetic colloid-polymer mixtures and with simulations show that "depletion" (or, equivalently, "macromolecular crowding") is the dominant mechanism: exclusion of the non-adsorbing polymer from the region between two neighbouring bacteria creates an unbalanced osmotic force pushing them together. The implications of our results for understanding phenomena such as biofilm formation are discussed.

Introduction. – Many species of bacteria secret high–molecular-weight polymers known as exopolysaccharides (EPS) into their aqueous surroundings [1]. EPS are important in various natural processes involving bacterial aggregation, including the establishment of biofilms on surfaces. Such phenomena are typically explained in the biological literature by invoking the supposed "stickiness" of EPS: a well-cited review being entitled "Biofilm exopolysaccharides: a strong and sticky framework" [2].

The vast majority of EPS are anionic polyelectrolytes [1], and most bacterial surfaces bear a net negative charge [3]. A dispersion of bacteria and anionic exopolysaccharides therefore constitutes a mixture of like-charge colloids and polymers. Compared to the case of opposite-charge mixtures, where simple electrostatics can give rise to polymer-induced bridging aggregation of the particles (whether colloids [4] or bacteria [5]), aggregation in like-charge colloid-polymer mixtures is far less understood.

In a like-charge colloid-polymer mixture, three generic mechanisms may be invoked to explain polymer-induced aggregation. Consider specifically anionic polyelectrolytes and colloids. First, the colloids (like most bacteria) may be amphoteric, and display a minority of positive charges. At low enough ionicity, the negative polymer segments may adopt loopy configurations to contact the positive surface patches [6], leading to bridging and aggregation. Secondly, polyvalent cations can form salt bridges between negatively charged particles and polymer, once again allowing polymer-induced bridging [7].

At high enough salt concentrations, a third mechanism can operate. Here, the Debye screening length (κ^{-1}) may become significantly smaller than the size of the colloids and polymers, but is still large enough to prevent van der Waals attraction. In such "marginally screened" mixtures, we have effectively neutral particles with the size increased by κ^{-1}, and slightly expanded polymer coils that are non-adsorbing to the particles. Exclusion of polymer from the region between two nearby particles leads to an unbalanced osmotic pressure pushing them together. The range of this inter-particle "depletion attraction" is controlled by the size of polymer coils, while its strength increases with the polymer concentration. Depletion aggregation is quantitatively understood in uncharged colloid-polymer mixtures [8], especially mixtures of hard-sphere colloids and near-ideal linear polymers [9]. Marginally screened like-charge colloid-polymer mixtures display qualitatively identical phenomenology [10].

(a) Present address: Université du Luxembourg - Luxembourg, EU.
(b) E-mail: w.poon@ed.ac.uk

In this letter, we present a study of like-charge bacteria-polymer mixtures in "marginally screened" phosphate buffer. To investigate whether depletion is generic, experiments were performed using two unrelated species of bacteria, a non-pathogenic strain of enteric *Escherichia coli* and the nitrogen-fixing bacterium *Sinorhizobium meliloti*, and two quite different anionic polyelectrolytes, synthetic sodium polystyrene sulfonate (NaPSS) and natural succinoglycan (SG) secreted by *S. meliloti*. NaPSS is a more-or-less globular, random-coil polymer under our experimental conditions [11], while SG is rod-like (with a persistence length of $\sim 150\,\mathrm{nm}$ in 0.1 M NaCl [12]). We used bacteria that have few or no flagella in order to establish the physics in the simplest possible model system: the presence of flagella would complicate the colloidal interaction between cells, and any motility will introduce new physics. But since flagella production is down-regulated in natural situations such as biofilm formation [13,14], our experimental systems are still of significant biological interest. Our measured phase diagrams and Monte Carlo simulations demonstrate that depletion is the most likely dominant mechanism causing aggregation in each of our four mixtures of non-flagellated bacteria and polymers.

Depletion effects are widely neglected in the biological literature on EPS-induced bacterial aggregation in general, and in considering the role of EPS in biofilm formation in particular (*e.g.*, depletion is not mentioned in [2].) Our results show that this position is highly questionable. In particular, since non-adsorbing polymers also cause a depletion attraction between particles and walls [15,16], it may be important in biofilm formation.

Experiments. – *E. coli* strain AB1157 and *S. meliloti* strain Rm1021 were both grown in Luria-Bertani (LB) broth at 30 °C to stationary phase, harvested by centrifugation, washed, and resuspended to any desired cell concentration in modified phosphate buffer (MPB)[1]. The cells and polymers were found to be individually stable in MPB. Electrophoretic mobility measurements (Malvern Zetasizer) confirmed that the bacteria carried a net negative charge. Note that MPB is *not* a medium for stimulating EPS secretion by either *E. coli* or *S. meliloti*, and plated colonies of either species grown in MPB did not appear mucoidal; we therefore assume that there was no significant EPS secretion under our conditions.

From electron microscopy, we know that our preparative procedure removed the vast majority of the flagella on cells of either species, leaving only a very small fraction still motile. Direct imaging shows that our *E. coli* AB1157 cells have average length and width of $L = 2 \pm 0.1\,\mu\mathrm{m}$ and $D = 1 \pm 0.1\,\mu\mathrm{m}$, and therefore an average aspect ratio of $L/D = 2$. Corresponding figures for *S. meliloti* Rm1021 were found to be $L = 1.7 \pm 0.3\,\mu\mathrm{m}$ and $D = 0.7 \pm 0.1\,\mu\mathrm{m}$, giving an aspect ratio of $L/D = 2.4$.

NaPSS was purchased from Aldrich and used as received. Gel permeation chromatography against PSS standards gave a molecular weight of $M_w = 64700\,\mathrm{g/mol}$ (polydispersity $M_w/M_n = 3.1$). Dynamic light scattering returned a hydrodynamic radius of $r_H = 8.7 \pm 0.1\,\mathrm{nm}$. The SG was harvested from an *exoS* mutant strain of *S. meliloti* derived from Rm 1021 (Rm 7096 [17]), which overproduces SG when grown in M9 medium [18]. Static light scattering data extrapolated to zero wavevector and concentration (Zimm plot) gave $M_w = 5.63 \pm 0.6 \times 10^5\,\mathrm{g/mol}$ and a radius of gyration of $r_g = 184 \pm 15\,\mathrm{nm}$.

Samples with various compositions were prepared in cuvettes, shaken to homogenise, and left for observation at 20 °C by direct visual inspection, time-lapse photography and optical density (OD) measurements.

Observed phase behaviour. – The effect of adding NaPSS to *E. coli* and *S. meliloti* Rm1021 was close to identical. We show and discuss results for for *E. coli* AB-1157 in detail, fig. 1. At zero and lowest polymer concentrations we observed a meniscus falling a few mm in 24 h, consistent with $\sim 1\,\mu\mathrm{m}$ objects having the density of *E. coli* ($\approx 1.08\,\mathrm{g/cm^3}$ [19]) sedimenting in phosphate buffer (density $\approx 1.00\,\mathrm{g/cm^3}$ [20]). In other words, we are seeing essentially single-cell sedimentation (thus confirming the colloidal stability of our cells in the phosphate buffer).

At each cell concentration, there was a critical polymer concentration above which samples became optically inhomogeneous, with a region denser in bacteria building up at the bottom. In fig. 1 this starts with sample 3 (see part (e) of this figure). As the polymer concentration increased, the phase separation process accelerated (compare samples 3 to 9 at different times in fig. 1).

In the first phase-separated sample shown in fig. 1(e) (cuvette 3), the upper, more dilute, phase clearly contains bacteria. In subsequent phase-separated samples (cuvettes 4–9), the upper phases are visually clear. However, optical density measurements (data not shown) confirmed the presence of bacteria in each of these upper phases, and that the concentration of bacteria in the upper phase decreased as the polymer concentration increased. Moreover, the amount of lower phase increased with increasing polymer concentration, fig. 1(e). Finally, we found total reversibility: the critical polymer concentration remained unchanged when we repeated our measurements after redispersing samples by gentle shaking. Taken together, these observations suggest that we are seeing equilibrium thermodynamic phase separation.

We therefore summarise our observations in the form of a phase diagram, fig. 2. Exactly the same phenomenology was observed if we used either a non-flagellated mutant of *E. coli* AB1157[2], or wild-type AB1157 that were prepared

[1] For *E. coli* AB1157 we used 6.2 mM K_2HPO_4, 3.8 mM KH_2PO_4, 66 mM NaCl, 0.1 mM EDTA at pH = 7.0; for *S. meliloti* we used 10 mM Na_2HPO_4, 2 mM NaH_2PO_4, 137 mM NaCl, 2.7 mM KCl. The ionicities ($I = \sum_i z_i^2 c_i$, where z_i is the charge on ionic species i in electronic units and c_i is its molar concentration) are 0.18 M and 0.34 M, respectively. The Debye screening lengths ($\approx 10\,\mathrm{nm}/\sqrt{I\,(\mathrm{mM})}$) are 0.8 nm and 0.5 nm.

[2] In this mutant, the gene for the basal ring of the flagella motor (*fliF*) is non-functional, so that no flagella are synthesized.

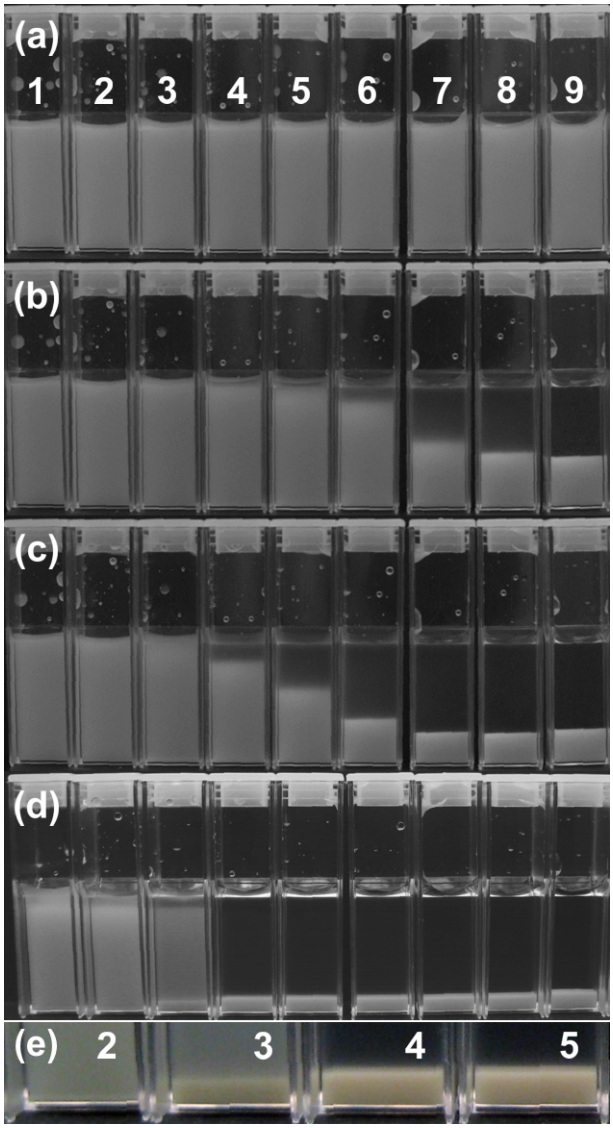

Fig. 1: (Colour on-line) Samples of viable *E. coli* AB1157 (cell density $= 1 \times 10^{11}$ cfu/ml, corresponding to a cell volume fraction of $\approx 13\%$) dispersed in phosphate buffer with NaPSS ($M_w = 64700$). The polymer weight fraction increases from left to right, with samples 1 to 9 containing 0%, 0.1%, 0.2%, 0.3%, 0.4%, 0.5%, 0.75%, 1% and 2% of NaPSS. Times: (a) $t = 0$, (b) $t = 30$ min, (c) $t = 100$ min, (d) $t = 24$ h. (e) A close-up of the lowest parts of samples 2–5 after 24 h. Sample 3 shows a small amount of denser, lower phase coexisting with a less dense upper phase. The lower phase volume increases with polymer concentration, but decreases in cell concentration: the upper phase in sample 4 already has no visible turbidity. (Note: parts (d) and (e) are best viewed on-line.)

as before but then rendered non-viable by heating to 60 °C for 30 minutes. The resulting phase diagrams are identical to fig. 2 to within experimental uncertainties. The same kind of phase separation behaviour was observed in mixtures of *S. meliloti* Rm1021 and NaPSS. The phase boundary is flat for the region of cell densities investigated, although it occurs at a somewhat higher polymer concentration (≈ 0.25 wt.% rather than ≈ 0.15 wt.%).

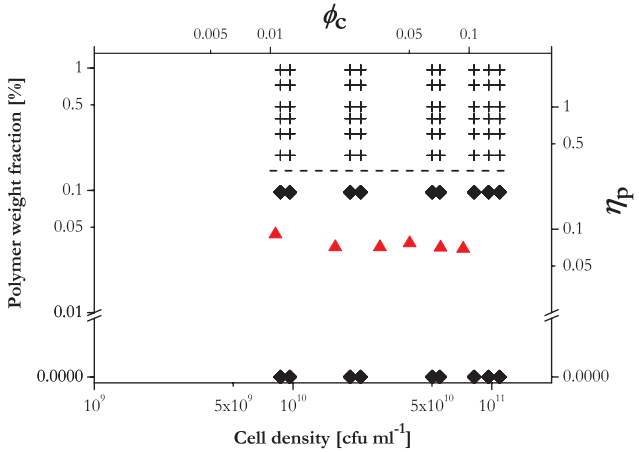

Fig. 2: (Colour on-line) Phase diagram for viable, deflagellated *E. coli* AB1157 in MPB with NaPSS ($M_w = 64700$). For cell and polymer volume fractions, ϕ_c and η_p, see footnote[3]. Note the logarithmic axes. ⧫: Single phase; +: two-phase coexistence. The dashed line indicates the approximate position of the equilibrium vapour-liquid phase boundary. To within experimental uncertainties, the observed phase diagrams for adding NaPSS to heat-treated non-viable, deflagellated *E. coli* and to the non-flagellated mutant (Δ*fliF*) are the same as the phase diagram shown here. ▲ (red) = simulated phase boundary.

When we changed the polymer from NaPSS to SG produced by *S. meliloti*, the observed phenomenology is again identical, but a large quantitative difference emerged: approximately an order of magnitude less polymer was needed to cause phase separation. Figure 3(a) shows the data for *S. meliloti* with SG. The phase boundary in the region of cell concentrations investigated now has an obvious negative slope. Results for SG with deflagellated *E. coli* AB1157 are similar, fig. 3(b).

Is it depletion? – Depletion-induced phenomena are well understood in mixtures of hard-sphere colloids and non-adsorbing random-coil polymers. In a nearly-monodisperse suspension with volume fraction $\lesssim 40\%$, adding sufficient polymer leads to fluid-crystal phase separation [9]. Buried in the fluid-crystal coexistence region of the phase diagram, there is a metastable vapour-liquid phase boundary [9]. Particles that are sufficiently polydisperse or non-spherical in shape will not be able to crystallize. In such a suspension where crystallization is suppressed, increasing polymer concentration gives rise to vapour-liquid phase separation instead [21]. If the particles are sufficiently anisotropic, adding polymer leads to coexistence of isotropic and nematic phases of the particles. For spherocylinders, this requires an aspect ratio (end-to-end length to diameter) of $\gtrsim 4$ [22,23].

Our *E. coli* and *S. meliloti* cells may be approximated as somewhat polydisperse spherocylinders of aspect ratio ≈ 2, which is too low for the occurrence of a nematic phase. If depletion is the dominant mechanism in our bacteria-polymer mixtures, we may therefore expect that adding polymer should give rise to vapour-liquid phase

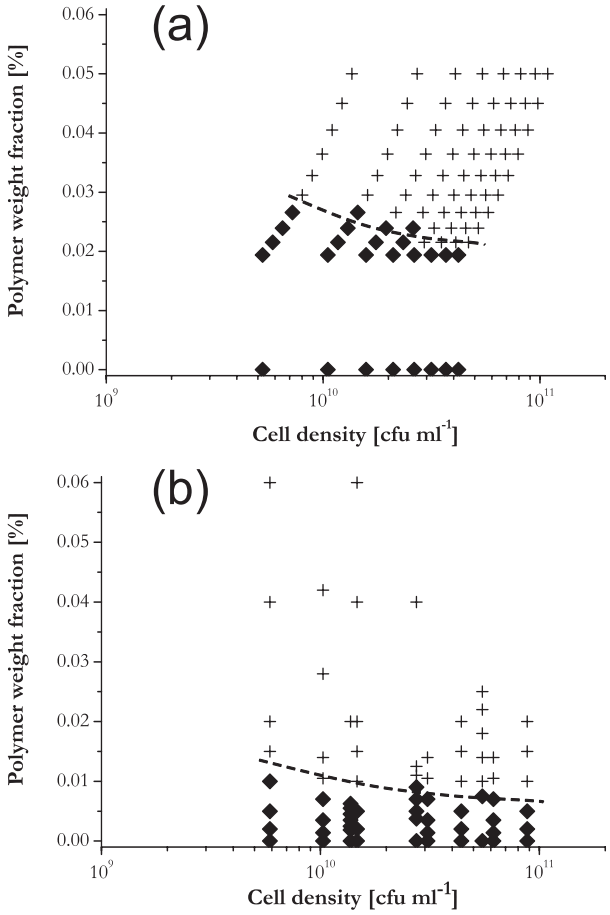

Fig. 3: The phase diagram of deflagellated (a) *S. meliloti* Rm1021 and (b) *E. coli* AB1157 in MPB with succinoglycan ($M_w = 563000$). Symbols are as in fig. 2.

separation, which is exactly what we observed, fig. 1. Qualitatively, therefore, there is *prima facie* evidence that phase separation in our mixtures is depletion-driven.

Quantitative evidence comes from comparing the amount of NaPSS and SG needed to cause phase separation, figs. 2 and 3. Literature data suggest that NaPSS is slightly non-ideal at the kind of ionicity we worked [11], so that we have somewhat expanded random coils. SG, however, is a semi-rigid rod [12]. Rods (length L, diameter D) are known to be much more effective depletants than random-coil polymers (radius r). Depletion-driven phase separation is essentially a manifestation of "macromolecular crowding" [24]: the depletant (polymer) "crowds out" the colloids to make room for themselves. A rod of length L rapidly reorienting in solution occupies an effective volume $\sim L^3$, *i.e.* it should be a comparable depletant to a polymer coil of diameter L. However, the rod's mass only scales linearly as L, while an equivalent polymer coil's mass scales as $L^{1/\nu}$ ($\nu = 0.5$ and 0.58 in ideal and good solvents, respectively). A lower mass of rods than coils is therefore needed to achieve the same degree of "crowding".

A crude quantitative estimate of this effect can be made by assuming that the depletion attraction between two particles at contact stays constant along the phase boundary and taking the cells as spheres. Analytic expressions are known for the contact depletion attraction for two spheres in a sea of ideal polymers approximated as spheres [25] and rods [26]. Using these expressions, and recalling that the length of a rod L is related to its radius of gyration r_g by $L = \sqrt{12} r_g$, we find that the weight fraction (wt%) ratio at phase separation is given by the expression:

$$\frac{\mathrm{wt\%\,(coils)}}{\mathrm{wt\%\,(rods)}} = \left(\frac{r_g^{(\mathrm{rods})}}{r_g^{(\mathrm{coils})}} \right)^2 \frac{M_w^{(\mathrm{coils})}}{M_w^{(\mathrm{rods})}}. \qquad (1)$$

This evaluates to ≈ 12 for our NaPSS and SG parameters. The almost exact agreement with the observed factor of ~ 12 drop in the phase boundary observed on going from fig. 2 to fig. 3(b) is no doubt fortuitous, but the order-of-magnitude agreement strongly supports our contention that "depletion" (or crowding) is the dominant mechanism in causing phase separation in our systems.

Note that more polymer (NaPSS or SG) is needed to phase separate *S. meliloti* than *E. coli*. This is consistent with the depletion potential between particles scaling as their (linear) size [25,26]: our *S. meliloti* cells are indeed smaller than our *E. coli* cells, although the $\sim 30\%$ difference does not account fully for the different phase boundaries.

Simulations. – Since depletion is a crowding effect, we expect that less polymer should be needed to cause phase separation at a higher concentration of bacteria. In other words, the slope of the phase boundary in phase diagrams such as those plotted in figs. 2 and 3 should be negative. Such negative-sloping phase boundaries are indeed seen in mixtures of synthetic hard-sphere colloids and non-adsorbing polymers [9]. The phase boundaries for SG + bacteria mixtures also have visibly negative slopes, fig. 3. However, the observed phase boundaries in the case of NaPSS appear to be flat (fig. 2 and data not shown for non-viable *E. coli* and viable *S. meliloti*).

To see whether depletion in systems like ours indeed gives rise a phase boundary with no visible negative slope in the region of our cell concentrations, we performed computer simulations within the framework of the Asakura-Oosawa (AO) model of colloid-polymer mixtures [27]. We took the bacteria to be monodisperse hard spherocylinders (diameter D, length L) of aspect ratio $L/D = 2$ (directly matching our *E. coli* but somewhat too low for our *S. meliloti*). Polymers were taken as interpenetrable spheres of radius r, the interpenetrability being an approximation of polymer coils in an ideal solvent. Each polymer "sphere" cannot approach closer than a distance r from the surface of a bacterium particle. To arrive at a value for r, we start from the measured hydrodynamic radius of $r_H = 8.7\,\mathrm{nm}$ for NaPSS. We estimate $r_g/r_H \approx 1.8$ for nearly ideal polymers of our polydispersity [28], and take the depletion layer thickness to be $2r_g/\sqrt{\pi}$ [29], arriving at a value of $2r = 35\,\mathrm{nm}$ for our AO polymer "spheres".

We used special techniques to deal with the large number of polymer "spheres" needed per spherocylinder. Configuration space was explored by local translation and rotation moves and by cluster moves in the NVT ensemble. In order to avoid checking for overlaps with spherocylinders at a distance larger than the range of interaction, we used cell systems. Due to the large size ratio we needed two systems of different cell size. Cells of the order of the spherocylinder diameter, D, were used for checking cylinder-cylinder overlaps. Separately, cells of the order of the diameter of the interpenetrable spheres, $2r$, were used for detection of sphere-spherocylinder overlaps.

As there is a high probability of generating overlaps with the surrounding spheres for every displacement of a spherocylinder over a distance on the order of D, standard translation and rotation moves lead to very small acceptance probabilities (or to very small displacements). In order to overcome this problem we developed a cluster move, in which the positions of spherocylinders and polymer "spheres" were swapped. Additionally, we employed a cluster move in which connected clusters of spherocylinders were moved collectively to overcome equilibration problems due to the very narrow and deep depletion potential between spherocylinders induced by "polymers".

Simulations with up to 6 million spheres were performed, which were computationally expensive (ca. one month of CPU time on an Intel(R) Xeon(R) CPU E5345 running at 2.33 GHz). We therefore could not compute free energy differences. Instead, we estimated the location of the phase boundary from the cluster size distribution, fig. 4. The continuous distribution in fig. 4(a) corresponds to a sample that remains single phase, while the twin-peaked distribution in fig. 4(b) we take as the signature of phase separation. We cannot access spherocylinder volume fractions below $\sim 1\%$ because of the very large number of polymer spheres such simulations entail.

At each spherocylinder concentration, we estimated the phase boundary to be midway between the single-phase sample with highest polymer concentration and the phase-separated sample with lowest polymer concentration. Results are shown in fig. 2[3]. Qualitatively, the phase boundary is indeed *flat* to within statistical uncertainties in the range of cell concentrations studied. This supports the claim that depletion is the dominant mechanism causing phase separation in our experiments.

Quantitatively, our simulated phase boundary is too low by about a factor of 4. Given the crudeness of our model, such quantitative discrepancy is not unexpected. In particular, some of this discrepancy is due to uncertainties in choosing a radius for the AO spheres to represent the polymers — the cube of this radius is needed to compare simulation data (expressed in terms of the volume fraction of polymer "spheres") to experimental data (expressed in terms of polymer mass fraction). In any case, the fact that the experimental phase boundary is higher than the simulated one provides evidence against any significant "stickiness" between polymers and bacterial cells.

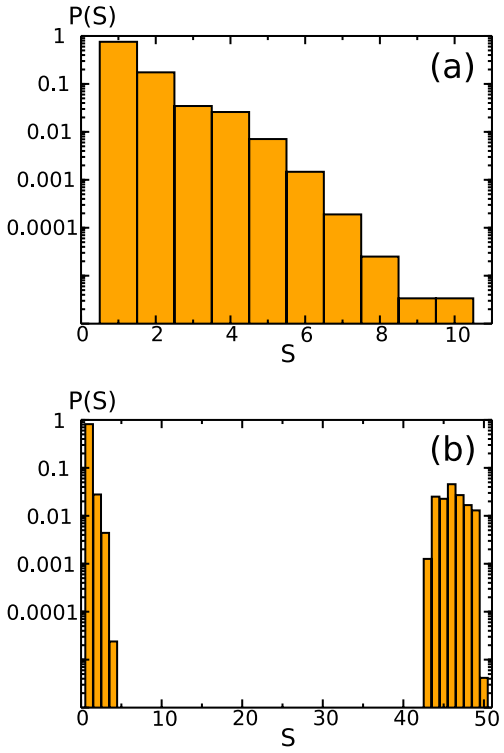

Fig. 4: (Colour on-line) Cluster size distributions. $P(S)$ gives the probability of encountering a cluster of size S. Note that the vertical scale is logarithmic. (a) $P(S)$ for a sample that we consider to be in the single-phase region of the phase diagram; the distribution is approximately exponential. (b) $P(S)$ for what we consider to be a phase-separated sample, displaying two peaks.

Conclusions. – We have provided experimental and simulational evidence that two anionic polyelectrolytes, one synthetic (NaPSS) and the other of natural origin (SG), induced phase separation in suspensions of two very different Gram-negative rod-shaped bacteria, *E. coli* and *S. meliloti*, by the depletion mechanism under marginally screened conditions. In other words, the ability of such anionic polyelectrolytes to aggregate bacteria is *not* due to stickiness, but is a consequence of "crowding".

Our results do not rule out specific mechanisms that may give rise to actual "stickness" between such polymers and bacterial surfaces. Stickiness will lead to bridging, and a phase boundary with *positive* slope: more polymers are required to bridge more bacteria. Such positive slope was indeed found in a previous study [31] in which NaPSS was added to *E. coli* in *distilled water*. With no added salt, screening is minimal and electrostatic interactions dominate, favouring the negative polymers "looping" to

[3]We convert between experimental and simulational concentration variables as follows. The cell density in cfu/ml multiplied by a cell volume of 1.3 μm^3 gives the cell volume fraction, ϕ_c, while the polymer weight (w_p) and volume (η_p) fractions are related by $w_p = \eta_p M_w/[\rho_0 N_A(4\pi r_g^3/3)]$, with ρ_0 being the density of the solvent (1 g/cm^3) and N_A is Avogadro's constant. Note that the latter procedure takes best account of polydispersity in the polymers [30].

contact minority positive patches on bacterial surfaces [6] and so bridging cells[4].

But this and other "stickiness" mechanisms (*e.g.*, polyvalent counterion bridging [7]) are specific to particular conditions or chemical species. Depletion, in contrast, is generic: it relies only on excluded volume, which is ubiquitous and cannot be "turned off". Our results therefore suggest that depletion should *always* be taken into account when bacteria are found in the presence of polymers. In particular, a population of EPS-secreting bacteria in a confined environment (*e.g.* a water drop) may generate enough polymer to cause phase separation. Moreover, it is interesting to speculate whether the rigidity of many EPS (xanthan from *Xanthomonas campestris* is another example [32]), which renders them highly effective depletants, is connected with their evolved biological function.

Since depletion also operates to induce an attraction between particles and surfaces [15,16], it may also play an important role in the initial stages of biofilm formation. Note that the deflagellated state of our cells may be of particular relevance here — the biofilm phenotype is often associated with down-regulation of flagella production (see [13] and [14] for *E. coli* and *S. meliloti* respectively).

Finally, it is interesting to ask, both as a question in physics and microbiology, what difference motility will make to the phenomena reported in this letter. The contact force due to depletion is easily estimated if we make a linear approximation of the depletion potential: $F_{\mathrm{dep}} \sim U_0/\delta$, where U_0 is the contact value of the attraction, and δ is its range. Take $U_0 \gtrsim k_B T$ at the phase boundary, while δ scales as the size of the polymer depletant. For our bacteria with NaPSS, therefore, $F_{\mathrm{dep}} \gtrsim k_B T/35\,\mathrm{nm} \sim 0.4\,\mathrm{pN}$. The flagella propulsion force in *E. coli* can be estimated using the Stokes formula for a sphere of radius a moving at constant speed v in a medium of viscosity η, $F_{\mathrm{prop}} \sim 6\pi\eta a v \sim 0.3\,\mathrm{pN}$ for $2a \sim 1\,\mu\mathrm{m}$ and $v \sim 30\,\mu\mathrm{m/s}$ [33] in water ($\eta \approx 10^{-3}\,\mathrm{Pa\,s}$), consistent with direct measurements [34]. Since $F_{\mathrm{dep}}/F_{\mathrm{prop}} \sim 1$, motility can significantly perturb depletion aggregation. The statistical mechanics of polymer-induced phase separation in such "active-particle suspensions" remains to be developed.

* * *

The EPSRC funded WCKP and JSL (EP/D071070/1), LGW and NTP (EP/E030173/1) and GD (studentship). We thank Dr G. P. Ferguson for *S. meliloti* strains. NaPSS was characterised at Rapra Technology.

REFERENCES

[1] Wingender J., Neu T. R. and Flemming H.-C., *Microbial Extracellular Polymeric Substances: Characterization, Structure and Function* (Springer) 1999.
[2] Sutherland I. W., *Microbiology*, **147** (2001) 3.
[3] Harden V. P. and Harris J. O., *J. Bacteriol.*, **65** (1953) 198.
[4] Furusawa K., Ueda M. and Nashima T., *Colloids Surf. A*, **153** (1999) 575.
[5] Harris R. H. and Mitchell R., *Ann. Rev. Microbiol.*, **27** (1973) 27.
[6] Hoda N. and Kumar S., *J. Chem. Phys.*, **128** (2008) 164907.
[7] Libera J. A., de la Cruz M. O. and Bedzyk M. J., *J. Phys. Chem. B*, **109** (2005) 23001.
[8] Asakura S and Oosawa F, *J. Chem. Phys.*, **22** (1954) 1255.
[9] Poon W. C. K., *J. Phys.: Condens. Matter*, **14** (2002) R859.
[10] Sperry P. R., *J. Colloid Interface Sci.*, **99** (1984) 97.
[11] Wang L. X. and Yu H., *Macromolecules*, **21** (1988) 3498.
[12] Dentini M., Crescenzi V., Fidanza M. and Coviello T., *Macromolecules*, **22** (1989) 954.
[13] Prignet-Combaret C., Vidal O., Dorel C. and Lejeune P., *J. Bacteriol.*, **181** (1999) 5993.
[14] Yao S.-Y., Luo L., Har K. J., Becker A., Rüberg S., Yu G.-Q., Zhu J.-B. and Cheng H.-P., *J. Bacteriol.*, **186** (2004) 6042.
[15] Dinsmore A. D., Warren P. B., Poon W. C. K. and Yodh A. G., *Europhys. Lett.*, **40** (1997) 337.
[16] Sear R. P., *Phys. Rev. E*, **57** (1998) 1983.
[17] Doherty D., Leigh J. A., Glazebrook J. and Walker G. C., *J. Bacteriol.*, **170** (1988) 4249.
[18] Sambrook J., Fritsch E. F. and Miniatis T., *Molecular Cloning: A Laboratory Manual*, Vol. **3** (Cold Spring Harbor Laboratory Press) 1989.
[19] Bailey J. E. and Ollis D. F., *Biochemical Engineering Fundamentals,* 2nd edition (McGraw Hill) 1986.
[20] Schiel J. E. and Hage D. S., *Talanta*, **65** (2005) 495.
[21] Fairhurst D. J., *Polydispersity in Colloidal Phase Transitions*, PhD Thesis, The University of Edinburgh (1999).
[22] Bolhuis P. G. and Frenkel D., *J. Chem. Phys.*, **107** (1997) 666.
[23] Bolhuis P. G., Stroobants A., Frenkel D. and Lekkerkerker H. N. W., *J. Chem. Phys.*, **107** (1997) 1551.
[24] Minton A. P., *Curr. Biol.*, **16** (2006) R269.
[25] Vrij A., *Pure Appl. Chem.*, **48** (1976) 471.
[26] Lin K., Crocker J. C., Zeri A. C. and Yodh A. G., *Phys. Rev. Lett.*, **87** (2001) 088301.
[27] Jungblut S., Tuinier R., Binder K. and Schilling T., *J. Chem. Phys.*, **127** (2007) 244909.
[28] Rubinstein M. and Colby R. H., *Polymer Physics* (Oxford University Press) 2003.
[29] Dehek H. and Vrij A., *J. Colloid Interface Sci.*, **88** (1982) 258.
[30] Warren P. B., *Langmuir*, **13** (1997) 4588.
[31] Eboigbodin K. E., Newton J. R. A., Routh A. F. and Biggs C. A., *Langmuir*, **21** (2005) 12315.
[32] Coviello T., Kajiwara K., Burchard W., Dentini M. and Crescenzi V., *Macromolecules*, **19** (1986) 2826.
[33] Berg H. C. and Brown D. A., *Nature*, **239** (1972) 500.
[34] Chattopadhyay S., Moldovan R., Yeung C. and Wu X. L., *Proc. Natl. Acad. Sci. U.S.A.*, **103** (2006) 13712.

[4]We also performed experiments in distilled water (data not shown), and found a positively sloping phase boundary.